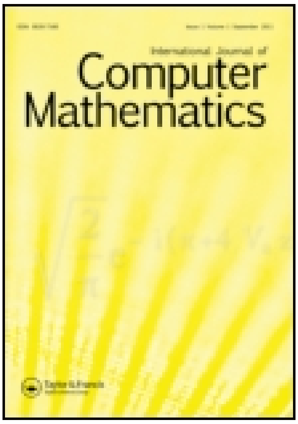

International Journal of Computer Mathematics
Publication details, including instructions for authors and subscription information:
http://www.tandfonline.com/loi/gcom20

Richardson extrapolation applied to boundary element method results in a Dirichlet problem for the Laplace equation

Shirley Pomeranz [a]

[a] Department of Mathematical and Computer Sciences, College of Engineering and Natural Sciences, The University of Tulsa, 800 S. Tucker Drive, Tulsa, OK, 74104-3189, USA

Available online: 28 Jun 2011

International Journal of Computer Mathematics
Vol. 88, No. 11, July 2011, 2306–2330

Richardson extrapolation applied to boundary element method results in a Dirichlet problem for the Laplace equation

Shirley Pomeranz*

Department of Mathematical and Computer Sciences, College of Engineering and Natural Sciences, The University of Tulsa, 800 S. Tucker Drive, Tulsa, OK 74104-3189, USA

(*Received 23 April 2010; revised version received 14 August 2010; accepted 1 November 2010*)

Richardson extrapolation is used to improve the accuracy of the numerical solutions for the normal boundary flux and for the interior potential resulting from the boundary element method. The boundary integral equations arise from a direct boundary integral formulation for solving a Dirichlet problem for the Laplace equation. The Richardson extrapolation is used in two different applications: (i) to improve the accuracy of the collocation solution for the normal boundary flux and, separately, (ii) to improve the solution for the potential in the domain interior. The main innovative aspects of this work are that the orders of dominant error terms are estimated numerically, and that these estimates are then used to develop an *a posteriori* technique that predicts if the Richardson extrapolation results for applications (i) and (ii) are reliable. Numerical results from test problems are presented to demonstrate the technique.

Keywords: boundary element method; collocation; Laplace equation; Richardson extrapolation

2000 AMS Subject Classifications: Primary 65B05; 65N35; 65N38; Secondary 35J05

1. Introduction

There are many papers that give results on topics such as enhancing the boundary element method with extrapolation, collocation convergence, and related error estimation for Fredholm integral equations of the first kind, on which this paper builds (e.g. [5,6,8,10–12]). However, new material presented in this paper provides an *a posteriori* estimator of the reliability of pointwise Richardson extrapolation approximations for the normal flux along the boundary of the domain and, similarly, for the primary unknown in the domain interior. The Richardson extrapolation is applied to improve the accuracy of the numerical solutions resulting from the boundary element method.

The problem of interest involves the numerical solution of an interior Dirichlet problem for Laplace's equation on a bounded domain in the plane. The domain may have a smooth boundary or may be a polygonal domain with corners. These two cases will be considered separately. The method of interest is a direct boundary integral method [7]. The boundary integral equations are discretized using collocation and then numerically solved for the unknown outward normal boundary flux (normal derivative of the primary unknown).

*Email: pomeranz@utulsa.edu

ISSN 0020-7160 print/ISSN 1029-0265 online

DOI: 10.1080/00207160.2010.537327
http://www.informaworld.com

For domains with smooth boundaries, the weakly singular boundary integral equation of the direct boundary integral method, which is a Fredholm integral equation of the first kind, is reformulated as an equivalent boundary integral equation of the second kind in order to use the Fredholm alternative theorem for the analysis of existence and uniqueness of solutions. Once the normal boundary flux is obtained, the problem can be solved for the potential in the domain interior (also referred to as the primary unknown).

- (i) In one application, the goals are to use Richardson extrapolation, even when the precise form of the error terms is not available, to obtain more accurate numerical approximations for the outward normal boundary flux and, in some sense, to be able to verify that the approximations are indeed more accurate.
- (ii) Analogously, in a separate application, Richardson extrapolation is used to obtain more accurate numerical approximations for the potential in the domain interior. Similarly, a goal is to be able to verify that these approximations are more accurate.

2. Problem statement and analysis

2.1 *Domains with smooth boundaries*

The first problem to be solved is the interior Dirichlet problem for Laplace's equation on D, a bounded domain in the plane with a smooth boundary, i.e. to find $u \in C(\bar{D}) \bigcap C^2(D)$ such that

$$\begin{aligned} \triangle u(P) &= 0, \quad P \in D, \\ u(P) &= u_0(P), \quad P \in \Gamma, \end{aligned} \tag{1}$$

where Γ is the boundary of domain D, and $u_0 \in C(\Gamma)$ is a given function. In this subsection, it is assumed that the boundary curve, Γ, is a simple, smooth, closed curve that can be parameterized by a C^2 function.

Using Green's identity and Green's representation formula yields the direct boundary integral equation, which involves the fundamental solution for Laplace's equation in the plane [3]:

$$u_0(P) = \frac{1}{\pi} \int_\Gamma \left(u_0(Q) \frac{\partial \ln |P-Q|}{\partial \mathbf{n}_Q} - \frac{\partial u(Q)}{\partial \mathbf{n}_Q} \ln |P-Q| \right) \mathrm{d}S_Q, \quad P \in \Gamma. \tag{2}$$

In order to emphasize the unknown quantity, $\partial u(Q)/\partial \mathbf{n}_Q$, the outward normal boundary flux, Equation (2) can be expressed using a single-layer potential boundary integral

$$\frac{1}{\pi} \int_\Gamma q(Q) \ln |P-Q| \, \mathrm{d}S_Q = g(P), \quad P \in \Gamma, \tag{3}$$

where

$$q(Q) \equiv \frac{\partial u(Q)}{\partial \mathbf{n}_Q} \quad \text{and} \quad g(P) \equiv -u_0(P) + \frac{1}{\pi} \int_\Gamma u_0(Q) \frac{\partial \ln |P-Q|}{\partial \mathbf{n}_Q} \, \mathrm{d}S_Q.$$

Equation (3) is a Fredholm integral equation of the first kind. Once Equation (3) is solved for q, the unknown normal boundary flux, then u, the unknown potential in the interior of domain D, can be determined using

$$u(P) = \frac{1}{2\pi} \int_\Gamma \left(u_0(Q) \frac{\partial \ln |P-Q|}{\partial \mathbf{n}_Q} - q(Q) \ln |P-Q| \right) \mathrm{d}S_Q, \quad P \in D. \tag{4}$$

It should be noted that the boundary integral equation (3) can be considered to be in $H^{-1/2}(\Gamma)$, where the single-layer potential operator is an elliptic operator, assuming suitable scaling. Then the Lax–Milgram theorem can be used to derive stability and error results for Lipschitz domains. Additionally, the Aubin–Nitsche trick can be used to obtain error estimates. These approaches are not used in this paper.

One method of analysis for a boundary integral equation of the first kind is, when possible, to represent the equation as an equivalent boundary integral equation of the second kind, and then apply the Fredholm alternative theorem for Fredholm integral equations of the second kind. That is how the issues of solution existence and uniqueness can be analysed. For completeness, this material, adapted from [1], is summarized now and culminates with Theorem 2.1.

The material in this paper includes some arguments from Anselone's work with collective compactness [1]. However, the results in Sections 4 and 5 are obtained under much less restrictive conditions, the trade-off being that weaker results are obtained. Although weaker, the results here are still useful: by using three Richardson extrapolations, explicit values for the rate of convergence are not required. Furthermore, a technique for predicting if numerical results are accurate will be obtained.

The equation of interest is Equation (3), where it is assumed that the boundary is not a 'Γ-contour' (equivalently, the logarithmic capacity is not equal to one). It has previously been assumed that Γ is a simple, smooth, closed curve that can be parameterized by a C^2 continuously differentiable function, $\mathbf{r}$. Under these assumptions, Equation (3) is uniquely solvable for all functions g in an appropriate function space.

As in [1], it is useful to simplify Equation (3) by parameterizing, i.e. standardizing the smooth position coordinate $\mathbf{r} \equiv \mathbf{r}(s) \equiv (\xi(s), \eta(s)) \in \Gamma$ and $|\mathbf{r}'(t)| \neq 0$ with parameters $s, t \in [0, 2\pi]$, and defining

$$\begin{aligned} P &\equiv \mathbf{r}(t), \\ Q &\equiv \mathbf{r}(s), \\ \mathrm{d}S_Q &\equiv \sqrt{\xi'(s)^2 + \eta'(s)^2}\,\mathrm{d}s, \\ \phi(s) &\equiv q(\mathbf{r}(s))\,|\mathbf{r}'(s)| = q(\mathbf{r}(s))\,\sqrt{\xi'(s)^2 + \eta'(s)^2}. \end{aligned} \tag{5}$$

The function ϕ represents a transformed form of q, the normal boundary flux. In order to prove that Equation (3) has a unique solution, first apply the parameterization (5), and then reformulate the integral in Equation (3) as

$$\begin{aligned} \frac{1}{\pi}\int_\Gamma q(Q)\ln|P-Q|\,\mathrm{d}S_Q &= \frac{1}{\pi}\int_0^{2\pi} \phi(s)\ln|\mathbf{r}(t)-\mathbf{r}(s)|\,\mathrm{d}s \\ &= \frac{1}{\pi}\int_0^{2\pi} \phi(s)\ln\left|2\mathrm{e}^{-1/2}\sin\left(\frac{t-s}{2}\right)\right|\,\mathrm{d}s \\ &\quad + \frac{1}{\pi}\int_0^{2\pi}\phi(s)b(t,s)\,\mathrm{d}s, \quad t \in [0, 2\pi], \end{aligned} \tag{6}$$

where

$$b(t,s) \equiv \begin{cases} \ln\left|\dfrac{\mathbf{r}(t)-\mathbf{r}(s)}{2\mathrm{e}^{-1/2}\sin((t-s)/2)}\right|, & \text{for } t-s \neq 2m\pi, \\ \ln|\mathrm{e}^{1/2}\mathbf{r}'(t)|, & \text{for } t-s = 2m\pi, \end{cases}$$

for $t \in [0, 2\pi]$ and where $m = 0, 1$. From Equations (3) and (6), this results in

$$\frac{1}{\pi}\int_0^{2\pi}\phi(s)\ln\left|2\mathrm{e}^{-1/2}\sin\left(\frac{t-s}{2}\right)\right|\,\mathrm{d}s + \frac{1}{\pi}\int_0^{2\pi}\phi(s)b(t,s)\,\mathrm{d}s = \bar{g}(t), \quad t \in [0, 2\pi], \tag{7}$$

where $\bar{g}$ is the transformed g due to the parameterization of the boundary,

$$\begin{aligned}\bar{g}(t) &\equiv g(\mathbf{r}(t)) \\ &= -u_0(\mathbf{r}(t)) + \frac{1}{\pi}\int_{\Gamma} u_0(\mathbf{r}(s)) \frac{\partial \ln|\mathbf{r}(t)-\mathbf{r}(s)|}{\partial \mathbf{n}_s} \frac{\partial \mathbf{n}_s}{\partial \mathbf{n}_Q} \sqrt{\xi'(s)^2+\eta'(s)^2}\,\mathrm{d}s.\end{aligned}$$

In operator form, Equation (7) can be expressed as

$$A\phi(t) + B\phi(t) = \bar{g}(t), \quad t \in [0, 2\pi], \tag{8}$$

with

$$\begin{aligned}A\phi(t) &\equiv \frac{1}{\pi}\int_0^{2\pi} \phi(s) \ln\left|2\mathrm{e}^{-1/2}\sin\left(\frac{t-s}{2}\right)\right| \mathrm{d}s, \quad t \in [0, 2\pi], \\ B\phi(t) &\equiv \frac{1}{\pi}\int_0^{2\pi} \phi(s) b(t,s)\,\mathrm{d}s, \quad t \in [0, 2\pi],\end{aligned}$$

where, for $r \geq 0$, $A : H^r[0, 2\pi] \to H^{r+1}[0, 2\pi]$ is an invertible bounded linear operator, $B : H^r[0, 2\pi] \to H^{r+1}[0, 2\pi]$ is a compact bounded linear operator, and $\bar{g} \in H^{r+1}[0, 2\pi]$. H^r denotes the usual Sobolev function space. In the material following Theorem 2.1, it is assumed that $r \geq 2$ so that the desired functions are smooth. In this form, the problem is to find $\phi \in H^r[0, 2\pi]$ that satisfies Equation (8).

The main purpose of reformulating Equation (3) as Equation (8) is to be able to express Equation (3), a Fredholm integral equation of the first kind, as an equivalent Fredholm integral equation of the second kind, which is given by

$$\begin{aligned}(I-K)\phi &= (I + A^{-1}B)\phi \\ &= A^{-1}\bar{g} \\ &= f,\end{aligned} \tag{9}$$

where I is the identity operator on $H^r[0, 2\pi]$, $K \equiv -A^{-1}B$ is a compact bounded linear operator on $H^r[0, 2\pi]$, and $f \equiv A^{-1}\bar{g} \in H^r[0, 2\pi]$. See [12, p. 561] for the Fourier series expression for A^{-1}. By the Fredholm alternative theorem, which applies to Equation (9) since Equation (9) is a Fredholm integral equation of the second kind and the boundary curve is not a ‘Γ-contour’, it follows that Equation (9) has a unique solution, $\phi \in H^r[0, 2\pi]$ for all $f \in H^r[0, 2\pi]$. Then Equations (3) and (4) have unique solutions, and therefore, Equation (1) has a unique solution.

The problem can now be discretized. The collocation method will be applied to Equation (9). For this purpose, the following notation will be used. P_n is the (piecewise) Lagrange interpolating polynomial projection operator that projects functions from a Banach space $V = H^r$ into V_n, an n-dimensional subspace of H^r. The functions in H^r are sufficiently smooth so that the projection operation makes sense. Sufficient smoothness is assumed so that the required entities exist. The piecewise Lagrange interpolating polynomials are of sufficiently low degree so that the Runge phenomena is not significant.

In order to use convenient operator notation that facilitates the error analysis, it is helpful to interpret collocation as a (piecewise) Lagrange interpolating polynomial projection of the residual, in which the interpolation nodes are chosen to be the collocation points (see below). The residual is piecewise interpolated at the collocation points, and this can be done since the value of the residual at these points is known, namely zero.

The piecewise Lagrange interpolation projection equation that approximates Equation (9) is

$$P_n(I-K)\phi_n = P_n f, \tag{10}$$

where $\phi_n \in V_n$ is the collocation approximation to $\phi \in V$. The collocation approximation is expressed as a linear combination of piecewise Lagrange basis functions $\{\psi_j\}_{j=1}^n$,

$$\phi_n(t) = \sum_{j=1}^{n} c_j \, \psi_j(t), \quad t \in [0, 2\pi].$$

In this subsection, it is assumed that $\{\psi_j\}_{j=1}^n$ are continuous functions on $[0, 2\pi]$.

The residual associated with ϕ_n is denoted by r_n,

$$\begin{aligned} r_n(t) &= (I - K)\phi_n(t) - f(t) \\ &= \phi_n(t) - \int_0^{2\pi} k(t,s)\phi_n(s)\,\mathrm{d}s - f(t) \\ &= \sum_{j=1}^{n} c_j \left(\psi_j(t) - \int_0^{2\pi} k(t,s)\psi_j(s)\,\mathrm{d}s \right) - f(t), \quad t \in [0, 2\pi], \end{aligned} \tag{11}$$

where k is the associated kernel. In the collocation method, n points are selected, t_i, $i = 1, \ldots, n$, and the system of equations generated by requiring that $r_n(t_i) = 0$, $i = 1, \ldots, n$, permits solution for the unknowns, c_j, $j = 1, \ldots, n$.

In this framework, using Equations (10) and (11), it follows that

$$r_n(t_i) = 0, \quad i = 1, \ldots, n,$$

if and only if

$$P_n(r_n) \equiv 0. \tag{12}$$

That is, the residual is zero at each collocation point, as required, if and only if the piecewise Lagrange interpolatory projection operator maps the residual to the zero function in the subspace. Formulation (12) (which is equivalent to Equation (10)) is the form that will now be used.

Theorem 2.1, modified only slightly from [1, pp. 346–349], is a collocation error bound theorem and applies to formulation (12) for the normal boundary flux.

THEOREM 2.1 *Assume that V is a Banach space with norm $\|\cdot\|$, $K : V \to V$ is a bounded linear operator, $I - K : V \to V$ is a bijective linear operator, and*

$$\|K - P_n K\| \longrightarrow 0 \quad as \quad n \longrightarrow \infty, \tag{13}$$

where I is the identity operator and $P_n : V \to V_n$ is the (piecewise) Lagrange interpolatory projection operator projecting into V_n, an n-dimensional subspace of V. Then, for all sufficiently large n, $n \geq N$, the operator $(I - P_n K)^{-1}$ exists as a uniformly bounded operator from V to V,

$$\sup_{n \geq N} \|(I - P_n K)^{-1}\| < \infty. \tag{14}$$

For the solutions ϕ and ϕ_n, with n sufficiently large, of Equations (9) *and* (10), *respectively, it follows that,*

$$\phi - \phi_n = (I - P_n K)^{-1}(\phi - P_n \phi), \tag{15}$$

and there is a two-sided error estimate,

$$\frac{1}{\|I - P_n K\|}\|\phi - P_n\phi\| \leq \|\phi - \phi_n\| \leq \|(I - P_n K)^{-1}\|\|\phi - P_n\phi\|. \tag{16}$$

Further, for n sufficiently large, the bounds in Equation (16) *can be made uniform in n,*

$$\frac{1}{\|I - K\| + \epsilon_N}\|\phi - P_n\phi\| \le \|\phi - \phi_n\| \le M\|\phi - P_n\phi\|, \quad n \ge N, \tag{17}$$

where ϵ_N and M are positive constants, independent of n.

Proof To prove Equation (14), use Equation (13) to choose N sufficiently large so that

$$\epsilon_N \equiv \sup_{n \ge N} \|(K - P_n K)\| < \frac{1}{\|(I - K)^{-1}\|}. \tag{18}$$

Then,

$$(I + (I - K)^{-1}(K - P_n K))^{-1}, \quad n \ge N,$$

exists and is uniformly bounded by the geometric series theorem for bounded linear operators. Using

$$\begin{aligned} I - P_n K &= (I - K) + (K - P_n K) \\ &= (I - K)(I + (I - K)^{-1}(K - P_n K)), \end{aligned}$$

the inverse and its bound are, respectively,

$$(I - P_n K)^{-1} = (I + (I - K)^{-1}(K - P_n K))^{-1}(I - K)^{-1},$$

$$\|(I - P_n K)^{-1}\| \le \frac{\|(I - K)^{-1}\|}{1 - \epsilon_N\|(I - K)^{-1}\|} \equiv M, \quad n \ge N, \tag{19}$$

where Equation (18) has been applied. The result (19) gives Equation (14).

To prove Equation (15), apply P_n to $(I - K)\phi = f$. Then, manipulate algebraically to obtain

$$(I - P_n K)\phi = P_n f + (\phi - P_n\phi). \tag{20}$$

From Equation (20), subtract

$$(I - P_n K)\phi_n = P_n f.$$

This yields

$$\begin{aligned} (I - P_n K)(\phi - \phi_n) &= (\phi - P_n\phi), \\ \phi - \phi_n &= (I - P_n K)^{-1}(\phi - P_n\phi), \quad n \ge N. \end{aligned} \tag{21}$$

Equation (21) is Equation (15).

To prove Equation (16), first take the norm in Equation (21), and then apply Equation (19) to obtain

$$\begin{aligned} \|\phi - \phi_n\| &= \|(I - P_n K)^{-1}(\phi - P_n\phi)\| \\ &\le M\,\|\phi - P_n\phi\|, \quad n \ge N. \end{aligned} \tag{22}$$

Inequality (22) proves that if $P_n\phi \to \phi$ as $n \to \infty$, then $\phi_n \to \phi$ as $n \to \infty$. This shows that the upper bound in Equation (16) follows directly from Equation (15). The lower bound follows by rearranging expressions and taking norms in Equation (21),

$$\frac{1}{\|I - P_n K\|}\|\phi - P_n\phi\| \le \|\phi - \phi_n\|, \quad n \ge N. \tag{23}$$

Results (22) and (23) give Equation (16). We have the result that $P_n\phi \to \phi$ as $n \to \infty$ is equivalent to $\phi_n \to \phi$ as $n \to \infty$; the two rates of convergence are the same.

Finally, to obtain Equation (17), note that from Equation (18)

$$\begin{aligned}\|I - P_n K\| &\leq \|I - K\| + \|K - P_n K\| \\ &\leq \|I - K\| + \epsilon_N, \quad n \geq N.\end{aligned} \tag{24}$$

Using Equation (24), the lower bound in Equation (16) can be replaced by

$$\frac{1}{\|I - K\| + \epsilon_N} \|\phi - P_n \phi\| \leq \|\phi - \phi_n\|. \tag{25}$$

Combining Equations (22) and (25) gives Equation (17), the desired two-sided uniform bound. ■

2.1.1 *Normal boundary flux for domains with smooth boundaries*

Theorem 2.1 will be used to justify the application of Richardson extrapolation to computing the outward normal boundary flux, q, in the case with smooth boundary and smooth functions and where Equation (5) relates q and ϕ. The basic assumptions here are that the domain boundary is smooth and that $r \geq 2$ so the desired functions are smooth. Unless indicated otherwise, the norm used for these functions is the sup-norm on $[0, 2\pi]$, denoted by $\| \cdot \|_\infty$. In order to justify the application of Richardson extrapolation with respect to computing the normal boundary flux, start with the following corollary to Theorem 2.1. This corollary provides a useful form for the normal boundary flux collocation error [1, 11.1.3, p. 350].

COROLLARY 2.2 *Under the hypotheses of Theorem* 2.1,

$$\phi - \phi_n = e_n^{(1)} + e_n^{(2)}, \tag{26}$$

where the two error terms are defined as

$$e_n^{(1)} = (I - K)^{-1}(\phi - P_n \phi), \tag{27}$$

$$e_n^{(2)} = \phi - \phi_n - e_n^{(1)}. \tag{28}$$

The norms of the error terms in Equations (27) *and* (28) *are related by*

$$\|e_n^{(2)}\| \leq \delta_n \|e_n^{(1)}\|, \quad \text{where } \delta_n \longrightarrow 0 \quad as \quad n \longrightarrow \infty. \tag{29}$$

Proof The proof consists of proving Equation (29). Using Equation (28) and (15) and simplifying gives

$$\begin{aligned} e_n^{(2)} &= \phi - \phi_n - e_n^{(1)} \\ &= \phi - \phi_n - (I - K)^{-1}(\phi - P_n \phi) \\ &= (I - P_n K)^{-1}(\phi - P_n \phi) - (I - K)^{-1}(\phi - P_n \phi) \\ &= [(I - P_n K)^{-1} - (I - K)^{-1}](\phi - P_n \phi) \\ &= [(I - P_n K)^{-1}(I - K) - I] \underbrace{(I - K)^{-1}(\phi - P_n \phi)}_{e_n^{(1)}}. \end{aligned} \tag{30}$$

Now, use the implicit definition of δ_n from Equation (30). Apply assumption (13) from Theorem 2.1 to

$$\begin{aligned} \delta_n &\equiv \|(I - P_n K)^{-1}(I - K) - I\| \\ &= \|(I - P_n K)^{-1}((I - K) - (I - P_n K))\| \end{aligned}$$

$$
\begin{aligned}
&= \|(I - P_n K)^{-1}(-K + P_n K)\| \\
&\le \|(I - P_n K)^{-1}\| \|(-K + P_n K)\| \\
&\le M\|(-K + P_n K)\| \longrightarrow 0, \quad \text{as} \quad n \longrightarrow \infty,
\end{aligned}
$$

where, from Theorem 2.1, M is a positive constant independent of n. This concludes the proof. ■

From Corollary 2.2, it follows that at each point in the parameterized boundary, $t \in [0, 2\pi]$, the collocation error for the normal boundary flux, $\phi(t) - \phi_n(t)$, has the form (26), which can be further expressed as

$$
\begin{aligned}
\phi(t) - \phi_n(t) &= e_n^{(1)}(t) + e_n^{(2)}(t) \\
&= (I - K)^{-1}(\phi - P_n\phi)(t) + e_n^{(2)}(t) \\
&= \sum_{j=0}^{\infty} K^j(\phi - P_n\phi)(t) + e_n^{(2)}(t) \qquad (31) \\
&= (\phi - P_n\phi)(t) + \sum_{j=1}^{\infty} K^j(\phi - P_n\phi)(t) + e_n^{(2)}(t). \qquad (32)
\end{aligned}
$$

In deriving Equation (32), the geometric series theorem for bounded linear operators has been applied to obtain the series expression for $(I - K)^{-1}$. It is assumed, for example, that there is sufficient smoothness with $\|K\| < 1$, and that the dominant error term is the $j = 0$ term from that series such that the remaining terms in the series are higher order error terms. Let the collocation approximation in Equation (32) be computed using a uniform mesh parameter (i.e. grid spacing), $h > 0$, with an associated n-dimensional approximation space. Similarly, using a refined uniform grid with a smaller grid spacing $\hat{h}$ and an associated $\hat{n}$-dimensional approximation space,

$$
\phi(t) - \phi_{\hat{n}}(t) = (\phi - P_{\hat{n}}\phi)(t) + \sum_{j=1}^{\infty} K^j(\phi - P_{\hat{n}}\phi)(t) + e_{\hat{n}}^{(2)}(t). \qquad (33)
$$

For the sake of exposition, a specific case will now be considered. The following material presented in this paper is an original work. It is assumed that quantities are sufficiently smooth so that piecewise Lagrange interpolation makes sense. Piecewise linear Lagrange interpolating polynomials are used here. Then, from Equations (32) and (33), and standard Lagrange interpolating polynomial error results,

$$
\begin{aligned}
\phi(t) - \phi_n(t) &= (t - t_i)(t - t_{i+1})\frac{\phi''(\xi_i(t))}{2} \\
&\quad + \sum_{j=1}^{\infty} K^j(\phi - P_n\phi)(t) + e_n^{(2)}(t) \\
&= \theta(\theta - 1)h^2\frac{\phi''(\xi_i(t))}{2} + \sum_{j=1}^{\infty} K^j(\phi - P_n\phi)(t) + e_n^{(2)}(t), \qquad (34)
\end{aligned}
$$

and, similarly,

$$
\phi(t) - \phi_{\hat{n}}(t) = (t - \widehat{t_i})(t - \widehat{t_{i+1}})\frac{\phi''(\hat{\xi}_i(t))}{2} + \sum_{j=1}^{\infty} K^j(\phi - P_{\hat{n}}\phi)(t) + e_{\hat{n}}^{(2)}(t)
$$

$$= \hat{\theta}(\hat{\theta}-1)\hat{h}^2\frac{\phi''(\hat{\xi}_i(t))}{2} + \sum_{j=1}^{\infty} K^j(\phi - P_{\hat{n}}\phi)(t) + e_{\hat{n}}^{(2)}(t)$$

$$\approx \hat{\theta}(\hat{\theta}-1)\hat{h}^2\frac{\phi''(\xi_i(t))}{2} + \sum_{j=1}^{\infty} K^j(\phi - P_{\hat{n}}\phi)(t) + e_{\hat{n}}^{(2)}(t), \tag{35}$$

where $0 \le \theta,\ \hat{\theta} \le 1$, $\xi_i(t) \in [t_i, t_{i+1}]$, and $\hat{\xi}_i(t) \in [\widehat{t_i}, \widehat{t_{i+1}}]$. It is assumed that ϕ is sufficiently smooth and h is sufficiently small so that $\phi''(\hat{\xi}_i(t)) \approx \phi''(\xi_i(t))$. Here, for $t \in [t_i, t_{i+1}]$,

$$t - t_i = \theta h,$$
$$t - t_{i+1} = -(1-\theta)h,$$

and similarly for the refined grid.

Since for t arbitrary, but fixed, h, $\hat{h}$, $\theta(t)$, and $\hat{\theta}(t)$ are known, the difference of the linear combination of Equation (34) multiplied by $\hat{\theta}(\hat{\theta}-1)\hat{h}^2$ and Equation (35) multiplied by $\theta(\theta - 1)h^2$ can be computed,

$$(\hat{\theta}(\hat{\theta}-1)\hat{h}^2(\phi(t)-\phi_n(t)) - \theta(\theta-1)h^2(\phi(t)-\phi_{\hat{n}}(t)))$$
$$= \hat{\theta}(\hat{\theta}-1)\hat{h}^2\left(\sum_{j=1}^{\infty} K^j(\phi - P_n\phi)(t) + e_n^{(2)}(t)\right)$$
$$- \theta(\theta-1)h^2\left(\sum_{j=1}^{\infty} K^j(\phi - P_{\hat{n}}\phi)(t) + e_{\hat{n}}^{(2)}(t)\right), \tag{36}$$

in which the dominant error terms have cancelled, as desired. The Richardson extrapolation approximation formula is obtained directly from Equation (36),

$$\phi(t) = \frac{\hat{\theta}(\hat{\theta}-1)\hat{h}^2\phi_n(t) - \theta(\theta-1)h^2\phi_{\hat{n}}(t)}{(\hat{\theta}(\hat{\theta}-1)\hat{h}^2 - \theta(\theta-1)h^2)}$$
$$+ \frac{1}{(\hat{\theta}(\hat{\theta}-1)\hat{h}^2 - \theta(\theta-1)h^2)}\left[\hat{\theta}(\hat{\theta}-1)\hat{h}^2\left(\sum_{j=1}^{\infty} K^j(\phi - P_n\phi)(t) + e_n^{(2)}(t)\right)\right.$$
$$\left. - \theta(\theta-1)h^2\left(\sum_{j=1}^{\infty} K^j(\phi - P_{\hat{n}}\phi)(t) + e_{\hat{n}}^{(2)}(t)\right)\right], \tag{37}$$

in which the first term on the right-hand side of Equation (37) is the Richardson extrapolation formula for the (transformed) normal boundary flux and the second term on the right-hand side consists of higher order error terms.

2.1.2 *Interior potential for domains with smooth boundaries*

The numerical technique described in this paper in Section 4 contrasts with the material in [10] for Robin boundary value problems for Laplace's equation for domains with smooth boundaries. In [10], a single-layer potential direct formulation is studied, and analysis is presented that justifies boundary element extrapolation and guarantees that extrapolated results for the boundary potential converge at a given rate. The trade-offs are that the results in the present paper are not as strong as those in [10], but they are more general and fewer restrictions are involved.

In order to justify the application of Richardson extrapolation with respect to computing u, the potential in the domain interior, recall Equation (4),

$$u(P) = \frac{1}{2\pi}\int_{\Gamma}\left(u_0(Q)\frac{\partial \ln|P-Q|}{\partial \mathbf{n}_Q} - q(Q)\ln|P-Q|\right)\mathrm{d}S_Q, \quad P \in D.$$

Let q_n be the collocation approximation to q on Γ and u_n be the associated approximation to u in D, computed using q_n. Using the same example as in Section 2.1.1 for ease of exposition, the results in this subsection follow directly from those in Section 2.1.1. Using Equations (4), (5), and (31), for $P \in D$, the following collocation error for the interior potential is obtained,

$$\begin{aligned}
u(P) - u_n(P) &= \frac{1}{2\pi}\int_{\Gamma}(q_n(Q) - q(Q))\ln|P-Q|\,\mathrm{d}S_Q \\
&= \frac{1}{2\pi}\int_0^{2\pi}(q_n(\mathbf{r}(s)) - q(\mathbf{r}(s)))\ln|P-\mathbf{r}(s)||\mathbf{r}'(s)|\,\mathrm{d}s \\
&= \frac{1}{2\pi}\int_0^{2\pi}(\phi_n(s) - \phi(s))\ln|P-\mathbf{r}(s)|\,\mathrm{d}s \\
&= \frac{1}{2\pi}\int_0^{2\pi}\left(\sum_{j=0}^{\infty}K^j(P_n\phi - \phi)(s) + e_n^{(2)}(s)\right)\ln|P-\mathbf{r}(s)|\,\mathrm{d}s \\
&= \frac{1}{2\pi}\int_0^{2\pi}((P_n\phi - \phi)(s))\ln|P-\mathbf{r}(s)|\,\mathrm{d}s \\
&\quad + \frac{1}{2\pi}\int_0^{2\pi}\left(\sum_{j=1}^{\infty}K^j(P_n\phi - \phi)(s) - e_n^{(2)}(s)\right)\ln|P-\mathbf{r}(s)|\,\mathrm{d}s \\
&= \frac{1}{2\pi}\int_0^{2\pi}((P_n\phi - \phi)(s))\ln|P-\mathbf{r}(s)|\,\mathrm{d}s + e_n^{(3)}(P),
\end{aligned} \tag{38}$$

where

$$e_n^{(3)}(P) \equiv \frac{1}{2\pi}\int_0^{2\pi}\left(\sum_{j=1}^{\infty}K^j(P_n\phi - \phi)(s) - e_n^{(2)}(s)\right)\ln|P-\mathbf{r}(s)|\,\mathrm{d}s$$

contains the higher order error terms. These higher order error terms are assumed to be less important than the $j = 0$ dominant error term. Discretize the boundary into n boundary elements,

$$e_i \equiv [s_i, s_{i+1}], \quad i = 1, \ldots, n,$$

where $s_1 \equiv s_{n+1}$. Using standard Lagrange interpolating polynomial error results with Equation (38) and the same example as in Section 2.1.1, piecewise linear Lagrange interpolating polynomials, gives

$$u(P) - u_n(P) = \frac{1}{2\pi}\sum_{i=1}^{n}\int_{s_i}^{s_{i+1}}(s - s_i)(s_{i+1} - s)\frac{\phi''(\xi_i(s))}{2}\ln|P-\mathbf{r}(s)|\,\mathrm{d}s + e_n^{(3)}(P). \tag{39}$$

With the assumptions that ϕ is sufficiently smooth and h is sufficiently small, it follows that on each element, $[s_i, s_{i+1}]$, ϕ'' has approximately a constant value, ϕ_i''. Further assume that the interior point $P \in D$ is bounded sufficiently away from the boundary so that on each element $[s_i, s_{i+1}]$, $\ln|P - \mathbf{r}(s)|$ has approximately a constant value, $\ln|P - \mathbf{r}_i|$. Observe that

$$\int_{s_i}^{s_{i+1}} (s - s_i)(s_{i+1} - s)\,\mathrm{d}s = \frac{h^3}{6}.$$

Under the given assumptions (or, equivalently, applying the weighted mean value theorem for integrals), Equation (39) gives

$$\begin{aligned} u(P) - u_n(P) &\approx \frac{1}{2\pi}\sum_{i=1}^{n}\left(\frac{h^3}{6}\right)\frac{\phi_i''}{2}\ln|P - \mathbf{r}_i| + e_n^{(3)}(P) \\ &= h^2\left(\frac{1}{24\pi}\right)\sum_{i=1}^{n}\phi_i''\ln|P - \mathbf{r}_i|h + e_n^{(3)}(P) \\ &\approx h^2\left(\frac{1}{24\pi}\right)\int_0^{2\pi}\phi''(s)\ln|P - \mathbf{r}(s)|\,\mathrm{d}s + e_n^{(3)}(P). \end{aligned} \tag{40}$$

Result (40) shows that, under the given assumptions, Richardson extrapolation can be applied to improve the numerical results for the interior potential. This general framework for the case in which there is sufficient smoothness can be contrasted with the following case in which the domain has corners.

2.2 *Domains with corners (polygonal domains)*

The numerical technique described in this paper in Sections 4 and 5 contrasts with the material in [8] for Dirichlet boundary value problems for Laplace's equation on polygonal domains. In [8], a double-layer potential, indirect formulation is studied. A graded mesh is used for a Galerkin method implementation with (standard and) multi-parameter extrapolation, and an analysis is presented that justifies boundary element extrapolation and guarantees that extrapolated results for the normal boundary flux and the potential in the domain interior converge at given rates. Again, the trade-offs are that the results in the present paper are not as strong as those in [8], but they are more general with fewer restrictions involved, and the results herein are new and useful in other ways.

2.2.1 *Normal boundary flux for domains with corners*

For the problem under consideration but with polygonal boundaries, specifically domains with corners, there is no guarantee that Richardson extrapolation will improve the numerical results since, without additional assumptions/restrictions, there is no convenient form for the dominant error term. However, domains with corners will be revisited in detail in Section 5 with a technique for dealing with Richardson extrapolation in this case.

2.2.2 *Interior potential for domains with corners*

Results for the convergence of collocation on a polygon, such as from [11, p. 153], suggest that the application of Richardson extrapolation could be beneficial. That result, which uses a uniform mesh,

$$|u(\tau) - u^h(\tau)| = O(h^{\beta+3/2}), \quad \tau \in D,$$

(at least) applies here with $\beta = -1/3$. In this notation from [11], u^h is the collocation approximation to u, the exact potential in the interior of D.

3. Brief comments on Richardson extrapolation

The object of Richardson extrapolation is to find a computationally inexpensive way to combine previously computed lower order (less accurate) numerical results in a way that produces formulas with higher order (more accurate) numerical results. It is stated that the method is extremely useful when there is a reliable estimate of the form of the discretization error as a function of the grid length [9]. However, even if such information is not available, under quite general conditions Richardson extrapolation can improve the accuracy of numerical results.

The following material is a brief description of Richardson extrapolation as used in this paper. Let q denote the unknown exact quantity that is desired. Let q_1 and q_2 denote two numerical approximations to q that are computed using the same formula (and at the same grid point) but with different, sufficiently small positive grid spacings, h_1 and h_2, respectively. If the dominant term in the discretization error is proportional to h^p, for some known positive number p, then we obtain

$$q - q_1 = Ah_1^p + \text{higher order terms}, \tag{41}$$

$$q - q_2 = Ah_2^p + \text{higher order terms}, \tag{42}$$

where A denotes a constant of proportionality. Taking a linear combination of Equations (41) and (42) and solving for q yields

$$q \approx \tilde{q} \equiv \frac{h_2^p q_1 - h_1^p q_2}{h_2^p - h_1^p}.$$

The Richardson extrapolation result is given by $\tilde{q}$.

If the value of p is unknown, three approximations, using grid spacings h_1, h_2, and h_3, respectively, can be used to obtain

$$q \approx \tilde{q} \equiv \frac{q_1 q_3 - q_2^2}{q_1 - 2q_2 + q_3}, \tag{43}$$

where it is assumed that $h_1/h_2 = h_2/h_3 \equiv c$, for some constant $c > 1$. Further, the order of the dominant error term can be approximated by

$$p \approx \frac{\ln((q_2 - q_1)/(q_3 - q_2))}{\ln c}. \tag{44}$$

To derive Equation (43) use the three approximations

$$q - q_i = Ah_i^p + \text{higher order terms}, \quad i = 1, 2, 3. \tag{45}$$

Use Equation (45) to eliminate the Ah_i^p terms, $i = 1, 2, 3$,

$$\frac{q - q_1}{q - q_2} \approx \frac{Ah_1^p}{Ah_2^p} = c^p \tag{46}$$

$$\frac{q - q_2}{q - q_3} \approx \frac{Ah_2^p}{Ah_3^p} = c^p, \tag{47}$$

where the higher order error terms are treated as negligible and where the condition that $h_1/h_2 = h_2/h_3 = c$ has been applied. Equate Equations (46) and (47) to obtain

$$\frac{q - q_1}{q - q_2} \approx \frac{q - q_2}{q - q_3}. \tag{48}$$

Finally, solve Equation (48) for q to obtain, as desired, Equation (43),

$$q \approx \tilde{q} \equiv \frac{q_1 q_3 - q_2^2}{q_1 - 2q_2 + q_3}.$$

To derive Equation (44) use the three approximations (45) in the form

$$q_1 + Ah_1^p \approx q_2 + Ah_2^p, \tag{49}$$

$$q_2 + Ah_2^p \approx q_3 + Ah_3^p. \tag{50}$$

Use Equations (49) and (50) to form

$$\frac{q_1 - q_2}{q_2 - q_3} \approx \frac{h_1^p - h_2^p}{h_2^p - h_3^p} = c^p, \tag{51}$$

where, again, the higher order error terms are treated as negligible and the condition that $h_1/h_2 = h_2/h_3 = c$ has been applied. Finally, solve Equation (51) for p to obtain, as desired, Equation (44),

$$p \approx \frac{\ln\left((q_2 - q_1)/(q_3 - q_2)\right)}{\ln c}.$$

In the numerical examples investigated in Section 5, the value of p is not known.

Richardson extrapolation is applied to the model problem. Using [2, Problem #16, p. 87], the Richardson extrapolation convergence can be described as if it were convergence from Aitken's $\triangle^2$ method. The convergence result is stated now.

THEOREM 3.1 *Suppose that the sequence of approximations $\{q_n\}_{n=1}^{\infty}$ converges to the limit q such that*

$$0 \le \lim_{n \longrightarrow \infty} \frac{q_{n+1} - q}{q_n - q} \equiv \lambda < 1,$$

for some constant λ. Then, the associated sequence of iterates $\{\tilde{q}_n\}_{n=1}^{\infty}$, where

$$\tilde{q}_n \equiv \frac{q_n q_{n+2} - q_{n+1}^2}{q_n - 2q_{n+1} + q_{n+2}}, \quad n = 1, 2, \ldots,$$

converges to q faster than $\{q_n\}_{n=1}^{\infty}$ in the sense that

$$\lim_{n \longrightarrow \infty} \frac{\tilde{q}_n - q}{q_n - q} = 0.$$

Now consider approximating the unknown quantity, for example, the normal boundary flux, q (or the interior potential), using three successive grid spacings, $h_1 > h_2 > h_3$, chosen sufficiently small. The approximations q_1, q_2, and q_3 are computed using h_1, h_2, and h_3, respectively, and are such that $(q_2 - q)/(q_1 - q) \approx (q_3 - q)/(q_2 - q)$. Further assume that the errors $q_i - q$, for $i = 1, 2, 3$, all have the same sign. Theorem 3.1 states that if q_1, q_2, and q_3 belong to the sequence converging to q as described, then Richardson extrapolation based on q_1, q_2, and q_3 will give a more accurate approximation.

4. Implementation of an *a posteriori* pointwise estimator of Richardson extrapolation reliability

Recall that the original problem to be solved is the interior Dirichlet problem for Laplace's equation (1), to find $u \in C(\bar{D}) \bigcap C^2(D)$ such that

$$\triangle u(P) = 0, \quad P \in D,$$
$$u(P) = u_0(P), \quad P \in \Gamma,$$

where Γ is the boundary of domain D and $u_0 \in C(\Gamma)$ is a given function. In Section 2.1, it was assumed that the boundary curve, Γ, was smooth and could be parameterized by a C^2 function. For the numerical experiments, the domain was selected to be the unit square, $D \equiv (0, 1) \times (0, 1)$. Therefore, the boundary of D is not smooth, and consequently, the resulting integral operator in the Fredholm integral equation (3) is not a compact operator. The theory from Section 2.1 does not apply. Nevertheless, it is still of interest to apply Richardson extrapolation (43) to boundary element results (Section 2.2).

Let p be the order of the dominant error term, as defined in Equations (41) and (42). One issue that should be resolved is how to determine if the Richardson extrapolation numerical results are valid. Numerical results for the p-value estimates (44) can be used to predict those grid points at which the Richardson extrapolation (and boundary element method) results are not accurate. The p-values should be positive numbers. The p-value estimates that are imaginary, negative, or small (relative to the neighbouring values) can be interpreted as warning flags, i.e. indicators that predict the grid points at which the Richardson extrapolation results are not accurate (relative to the neighbouring results).

Note that determination if the p-value is too small is actually problem-dependent and somewhat subjective. In cases for which additional information about the solution is available, this information can be used to determine a cut-off for acceptable p-values. An 'educated' trial and error process, based on available numerical results and other data, can be used to select cut-offs for acceptable p-values. These values are not accurate either due to the boundary element method approximations themselves being inaccurate (e.g. near corners of the domain) or due to the Richardson extrapolation being inaccurate (e.g. if the grid spacings are too large). One possible remedy for these situations is to further refine the grid near grid points at which the p-value estimates are bad. The following issue is to be emphasized. For problems with or even without the underlying theory (i.e. in situations where this theory may not be known to the researcher), if numerical p-value estimates are complex with non-zero imaginary parts, are negative real numbers, or are of 'inappropriate' magnitude for a given problem, then, certainly, the Richardson extrapolation results at such grid points are unreliable (not valid) and should be discarded. This is new information that is gained by the use of the proposed technique. To paraphrase this, it is in the contrapositive sense to the following fact that the presented results are useful: if the Richardson extrapolation results are valid, then the order of the dominant error term, p, must be real, positive, and of 'appropriate' magnitude (e.g. based on any supplemental information that the researcher may have). Therefore, the contrapositive form of this statement, which applies even in the absence of the researcher's knowledge of the underlying theoretical properties of the problem, does indeed give us a useful result. We have a rejection criterion. We cannot say with certainty that some Richardson extrapolation results are good; but we can say with certainty that specific Richardson extrapolation results are bad.

For the purposes of describing the numerical experiments reported here, the following terminology is used. A 'bad Richardson extrapolation value' at a grid point (either on the boundary, when the normal boundary flux is of interest; or in the interior, when the potential (primary unknown) is of interest) is one for which the fine grid result is more accurate than the Richard extrapolation result. This means that the error magnitude for the fine grid result is smaller than that for the Richardson extrapolation result, which should not be the case.

Similarly, a 'bad p-value' at a grid point (either on the boundary or in the interior) is one that is complex (with non-zero imaginary part), negative, or too small. Since the p-value estimate is the numerically approximated order of the dominant error term, it should be a positive number, and not too small in regions for which the solution is reasonably smooth.

The *bad Richardson extrapolation values* are known in Section 5, since test problems with known exact solutions for both the normal boundary flux and the interior potential are used. However, in applications the *bad Richardson extrapolation values* would not be known, and the *bad p-values*, which are known, would be used as warning flags, i.e. predictors of points with poor Richardson extrapolation results.

5. Numerical experiments

5.1 *A first test problem*

The first test problem chosen for the model problem (1) has the exact solution

$$u(x, y) = \pi e^{y} \cos\left(x - \frac{\pi}{7}\right) + e^{(1-\pi x)} \cos\left(\pi y - \frac{\pi}{2}\right) + \frac{1}{100}\pi e^{5x} \cos\left(5y - \frac{\pi}{2}\right).$$

The domain is the square $D = \{(x, y)| \quad 0 < x < 1, \quad 0 < y < 1\}$. The Dirichlet boundary data used were that given on the boundary by the exact solution. A *Mathematica*© notebook implementing the boundary element method was written by the author of this paper. The *Mathematica* notebook implemented collocation in the classical direct boundary element method [4]. Piecewise constant (discontinuous) elements (basis functions) for the primary variable and its normal boundary flux were used. The collocation points were selected as the midpoints of each element (subinterval) in a uniform element grid on the boundary of the square. Note that the geometry nodes that delineate the end points of each boundary element are different from the collocation nodes, which are at the element midpoints. The boundary nodes were numbered sequentially, counterclockwise from the lower left vertex.

Initially, a relatively coarse uniform geometry grid was used on the boundary. The number of geometry x-nodes on a horizontal edge of the square domain was set equal to the number of geometry y-nodes on a vertical edge, denoted by nxnodes and nynodes, respectively. The boundary grid was then uniformly refined in such a way so as to have the collocation nodes in the coarse boundary grid remain as collocation nodes in the two other grids, the refined grids, that were used to construct the Richardson extrapolation results. The numbers of boundary geometry nodes were taken successively as nxnodes = nynodes = 10, 28, and 82, respectively, for the coarse, intermediate, and fine boundary grids. Each successive value of nxnodes (and nynodes) was computed by the formula

$$\text{current number of nxnodes} = 3(\text{previous number of nxnodes} - 1) + 1.$$

This formula for the boundary grids ensures that the 36 collocation nodes in the coarse boundary grid will also be collocation nodes in the successively refined boundary grids. Equivalently, each boundary element is uniformly trisected by successive Richardson refinements.

The interior grid is similarly refined for Richardson extrapolation of the interior potential values, where there is a 9×9 interior coarse grid (81 interior nodes). The 81 interior nodes were numbered sequentially from the lower left, from left to right and then from bottom to top. The additional amount of computer execution time to perform the Richard extrapolation (on the boundary and in the interior) is negligible compared with the execution time for a fine grid solution.

The focus of the numerical results that will now be described is (i) to use Richardson extrapolation to improve the numerical results for the normal outward boundary flux and, separately, (ii) to use Richardson extrapolation to improve the numerical results for the interior potential (primary unknown). A main interest in both (i) and (ii) is to be able to get information on the validity of these Richardson extrapolation results, especially since precise values of the parameters involved in the error terms are not assumed to be known.

5.1.1 *Richardson extrapolation for the first test problem normal boundary flux*

The numerical results for the normal boundary flux errors (not relative errors) computed with the coarse grid (nxnodes = nynodes = 10), intermediate grid (nxnodes = nynodes = 28), fine grid (nxnodes = nynodes = 82), and associated Richardson extrapolation and the resulting numerical estimates for the p-values are given in Table 1.

Table 1. Table of normal boundary flux errors and p-estimates for the first test problem, $u(x, y) = \pi e^{y} \cos(x - \pi/7) + e^{(1-\pi x)} \cos(\pi y - \pi/2) + (1/100)\pi e^{5x} \cos(5y - \pi/2)$.

	Normal boundary flux errors				
	nxnodes				
Node #	10	28	82	Richardson extrapolation	p-Estimate
1	-1.01×10^{1}	-8.79	-8.93	-8.91	$\mathbf{2.04 + 2.86\,i}$
2	1.76×10^{-1}	1.23×10^{-2}	1.94×10^{-3}	1.24×10^{-3}	2.51
3	3.95×10^{-2}	6.29×10^{-3}	9.06×10^{-4}	-1.35×10^{-4}	1.66
4	3.39×10^{-2}	4.36×10^{-3}	5.89×10^{-4}	3.78×10^{-5}	1.87
5	3.15×10^{-2}	3.95×10^{-3}	5.18×10^{-4}	2.98×10^{-5}	1.90
6	3.80×10^{-2}	4.75×10^{-3}	6.27×10^{-4}	4.34×10^{-5}	1.90
7	5.03×10^{-2}	7.35×10^{-3}	1.01×10^{-3}	-8.60×10^{-5}	1.74
8	1.95×10^{-1}	1.46×10^{-2}	2.17×10^{-3}	1.25×10^{-3}	2.44
9	-8.43	-7.18	-7.32	-7.31	$\mathbf{2.03 + 2.86\,i}$
10	1.06×10^{-1}	7.87×10^{-2}	1.24×10^{-2}	$\mathbf{1.25 \times 10^{-1}}$	$\mathbf{-0.81}$
11	1.29×10^{-1}	1.73×10^{-2}	2.40×10^{-3}	1.11×10^{-4}	1.84
12	9.81×10^{-2}	1.31×10^{-2}	1.63×10^{-3}	-1.49×10^{-4}	1.82
13	8.34×10^{-2}	1.07×10^{-2}	1.27×10^{-3}	-1.25×10^{-4}	1.86
14	5.36×10^{-2}	6.66×10^{-3}	7.68×10^{-4}	-7.78×10^{-5}	1.89
15	1.37×10^{-2}	1.41×10^{-3}	1.45×10^{-4}	2.67×10^{-7}	2.07
16	-3.04×10^{-2}	-3.66×10^{-3}	-4.32×10^{-4}	9.20×10^{-6}	1.93
17	3.48×10^{-2}	-6.67×10^{-3}	-6.97×10^{-4}	$\mathbf{-1.45 \times 10^{-3}}$	$\mathbf{1.76 + 2.86\,i}$
18	-1.25	8.84×10^{-2}	-3.31×10^{-4}	$\mathbf{5.20 \times 10^{-3}}$	$\mathbf{2.47 + 2.86\,i}$
19	1.93×10^{1}	1.81×10^{1}	1.81×10^{1}	1.81×10^{1}	$\mathbf{2.66 + 2.86\,i}$
20	-7.80×10^{-2}	-5.18×10^{-4}	-1.44×10^{-4}	-1.42×10^{-4}	4.85
21	3.86×10^{-3}	-5.88×10^{-4}	-1.48×10^{-4}	$\mathbf{-1.88 \times 10^{-4}}$	$\mathbf{2.11 + 2.86\,i}$
22	5.40×10^{-3}	5.28×10^{-5}	-7.10×10^{-5}	$\mathbf{-7.39 \times 10^{-5}}$	3.43
23	1.11×10^{-2}	7.30×10^{-4}	1.33×10^{-5}	$\mathbf{-3.98 \times 10^{-5}}$	2.43
24	1.72×10^{-2}	1.55×10^{-3}	1.21×10^{-4}	-2.21×10^{-5}	2.18
25	2.44×10^{-2}	2.79×10^{-3}	2.96×10^{-4}	-2.79×10^{-5}	1.97
26	5.87×10^{-2}	5.48×10^{-3}	7.22×10^{-4}	2.55×10^{-4}	2.20
27	3.76	3.98	3.95	$\mathbf{3.951}$	$\mathbf{1.86 + 2.86\,i}$
28	-4.97×10^{-1}	5.02×10^{-2}	3.59×10^{-3}	$\mathbf{7.25 \times 10^{-3}}$	$\mathbf{2.24 + 2.86\,i}$
29	7.14×10^{-2}	4.89×10^{-3}	7.03×10^{-4}	4.23×10^{-4}	2.52
30	3.41×10^{-2}	4.51×10^{-3}	5.44×10^{-4}	-7.09×10^{-5}	1.83
31	4.20×10^{-2}	5.04×10^{-3}	5.81×10^{-4}	-2.99×10^{-5}	1.93
32	4.60×10^{-2}	5.55×10^{-3}	6.46×10^{-4}	-3.02×10^{-5}	1.92
33	4.89×10^{-2}	6.08×10^{-3}	7.41×10^{-4}	-1.87×10^{-5}	1.90
34	5.52×10^{-2}	7.41×10^{-3}	9.82×10^{-4}	-1.63×10^{-5}	1.83
35	9.22×10^{-2}	1.35×10^{-2}	1.98×10^{-3}	-3.43×10^{-6}	1.75
36	2.30×10^{-1}	7.89×10^{-2}	1.32×10^{-2}	$\mathbf{-3.72 \times 10^{-2}}$	**0.76**

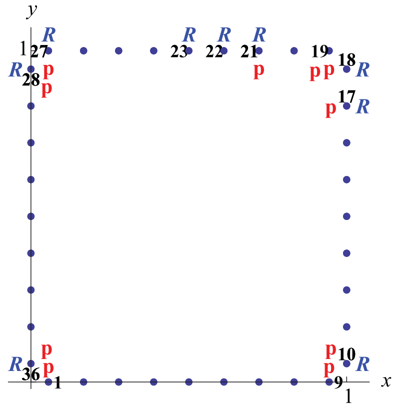

Figure 1. Boundary flux nodes at which the Richardson extrapolation normal boundary flux is bad (R), compared with boundary nodes at which the p-values predict bad Richardson extrapolation results (p) for the first test problem, $u(x, y) = \pi e^y \cos(x - \pi/7) + e^{(1-\pi x)} \cos(\pi y - \pi/2) + (1/100)\pi e^{5x} \cos(5y - \pi/2)$.

The numerical results for the normal boundary flux obtained from executing the *Mathematica* boundary element notebook three times, using the coarse, intermediate, and refined boundary grids, are compared with the Richardson extrapolation result that is computed using these three data sets. These four numerical approximations for the normal boundary flux are then compared with the exact solution values at the selected boundary flux nodes. Specifically, the Richardson extrapolation results should be compared with the results from the fine grid to see which are

Table 2. Table of interior potential errors and p-estimates for the first test problem, $u(x, y) = \pi e^y \cos(x - \pi/7) + e^{(1-\pi x)} \cos(\pi y - \pi/2) + (1/100)\pi e^{5x} \cos(5y - \pi/2)$.

Interior potential errors					
	nxnodes				
Node #	10	28	82	Richardson extrapolation	p-Estimate
1	8.62×10^{-4}	-1.94×10^{-4}	-1.49×10^{-5}	$\mathbf{-4.08 \times 10^{-5}}$	**1.62 + 2.86 i**
2	-2.40×10^{-3}	-1.60×10^{-4}	-1.59×10^{-5}	-5.93×10^{-6}	2.50
3	-1.44×10^{-3}	-1.49×10^{-4}	-1.53×10^{-5}	1.78×10^{-7}	2.06
4	-1.35×10^{-3}	-1.43×10^{-4}	-1.49×10^{-5}	3.92×10^{-7}	2.04
5	-1.36×10^{-3}	-1.44×10^{-4}	-1.50×10^{-5}	4.54×10^{-7}	2.04
6	-1.50×10^{-3}	-1.55×10^{-4}	-1.59×10^{-5}	-5.19×10^{-9}	2.07
7	-1.83×10^{-3}	-1.79×10^{-4}	-1.81×10^{-5}	-6.83×10^{-7}	2.12
8	-3.21×10^{-3}	-2.27×10^{-4}	-2.22×10^{-5}	-7.11×10^{-6}	2.44
9	-1.61×10^{-4}	-3.29×10^{-4}	-2.83×10^{-5}	$\mathbf{-2.21 \times 10^{-4}}$	**−0.53 + 2.86 i**
10	-2.31×10^{-3}	-2.94×10^{-4}	-3.11×10^{-5}	8.54×10^{-6}	1.85
11	-2.92×10^{-3}	-2.66×10^{-4}	-2.76×10^{-5}	-4.24×10^{-6}	2.20
12	-2.57×10^{-3}	-2.38×10^{-4}	-2.48×10^{-5}	-3.49×10^{-6}	2.18
13	-2.37×10^{-3}	-2.22×10^{-4}	-2.33×10^{-5}	-2.95×10^{-6}	2.16
14	-2.39×10^{-3}	-2.24×10^{-4}	-2.34×10^{-5}	-2.95×10^{-6}	2.17
15	-2.67×10^{-3}	-2.47×10^{-4}	-2.58×10^{-5}	-3.45×10^{-6}	2.18
16	-3.35×10^{-3}	-3.05×10^{-4}	-3.16×10^{-5}	-4.67×10^{-6}	2.19
17	-4.61×10^{-3}	-4.17×10^{-4}	-4.32×10^{-5}	-6.54×10^{-6}	2.20
18	-4.80×10^{-3}	-6.12×10^{-4}	-6.43×10^{-5}	1.80×10^{-5}	1.85
19	-3.44×10^{-3}	-4.49×10^{-4}	-4.82×10^{-5}	1.39×10^{-5}	1.83
20	-3.72×10^{-3}	-3.65×10^{-4}	-3.87×10^{-5}	-3.73×10^{-6}	2.12
21	-3.24×10^{-3}	-3.12×10^{-4}	-3.31×10^{-5}	-3.64×10^{-6}	2.14
22	-2.97×10^{-3}	-2.85×10^{-4}	-3.01×10^{-5}	-3.40×10^{-6}	2.14
23	-2.95×10^{-3}	-2.82×10^{-4}	-2.97×10^{-5}	-3.43×10^{-6}	2.15
24	-3.25×10^{-3}	-3.08×10^{-4}	-3.23×10^{-5}	-3.87×10^{-6}	2.16

(*Continued*)

Table 2. Continued

	Interior potential errors				
	nxnodes				
Node #	10	28	82	Richardson extrapolation	p-Estimate
25	-4.00×10^{-3}	-3.78×10^{-4}	-3.97×10^{-5}	-4.81×10^{-6}	2.16
26	-5.47×10^{-3}	-5.24×10^{-4}	-5.51×10^{-5}	-6.07×10^{-6}	2.14
27	-6.13×10^{-3}	-8.05×10^{-4}	-8.55×10^{-5}	2.71×10^{-5}	1.82
28	-4.18×10^{-3}	-5.51×10^{-4}	-5.93×10^{-5}	1.78×10^{-5}	1.82
29	-4.35×10^{-3}	-4.33×10^{-4}	-4.63×10^{-5}	-3.87×10^{-6}	2.11
30	-3.70×10^{-3}	-3.63×10^{-4}	-3.87×10^{-5}	-3.69×10^{-6}	2.12
31	-3.33×10^{-3}	-3.25×10^{-4}	-3.45×10^{-5}	-3.50×10^{-6}	2.13
32	-3.22×10^{-3}	-3.12×10^{-4}	-3.31×10^{-5}	-3.48×10^{-6}	2.13
33	-3.39×10^{-3}	-3.26×10^{-4}	-3.45×10^{-5}	-3.74×10^{-6}	2.14
34	-3.95×10^{-3}	-3.80×10^{-4}	-4.01×10^{-5}	-4.35×10^{-6}	2.14
35	-5.18×10^{-3}	-5.03×10^{-4}	-5.32×10^{-5}	-5.36×10^{-6}	2.13
36	-5.75×10^{-3}	-7.57×10^{-4}	-8.04×10^{-5}	2.55×10^{-5}	1.82
37	-4.40×10^{-3}	-5.79×10^{-4}	-6.23×10^{-5}	1.86×10^{-5}	1.82
38	-4.56×10^{-3}	-4.57×10^{-4}	-4.89×10^{-5}	-3.95×10^{-6}	2.10
39	-3.87×10^{-3}	-3.83×10^{-4}	-4.09×10^{-5}	-3.67×10^{-6}	2.11
40	-3.45×10^{-3}	-3.40×10^{-4}	-3.63×10^{-5}	-3.40×10^{-6}	2.12
41	-3.23×10^{-3}	-3.17×10^{-4}	-3.37×10^{-5}	-3.24×10^{-6}	2.12
42	-3.16×10^{-3}	-3.09×10^{-4}	-3.28×10^{-5}	-3.23×10^{-6}	2.12
43	-3.26×10^{-3}	-3.18×10^{-4}	-3.37×10^{-5}	-3.40×10^{-6}	2.13
44	-3.69×10^{-3}	-3.59×10^{-4}	-3.80×10^{-5}	-3.80×10^{-6}	2.13
45	-3.67×10^{-3}	-4.73×10^{-4}	-5.01×10^{-5}	1.44×10^{-5}	1.84
46	-4.06×10^{-3}	-5.29×10^{-4}	-5.68×10^{-5}	1.61×10^{-5}	1.83
47	-4.34×10^{-3}	-4.32×10^{-4}	-4.62×10^{-5}	-3.90×10^{-6}	2.11
48	-3.78×10^{-3}	-3.74×10^{-4}	-4.00×10^{-5}	-3.56×10^{-6}	2.11
49	-3.39×10^{-3}	-3.37×10^{-4}	-3.60×10^{-5}	-3.17×10^{-6}	2.11
50	-3.09×10^{-3}	-3.08×10^{-4}	-3.29×10^{-5}	-2.83×10^{-6}	2.11
51	-2.76×10^{-3}	-2.76×10^{-4}	-2.95×10^{-5}	-2.51×10^{-6}	2.11
52	-2.29×10^{-3}	-2.28×10^{-4}	-2.43×10^{-5}	-2.18×10^{-6}	2.11
53	-1.55×10^{-3}	-1.49×10^{-4}	-1.58×10^{-5}	-1.72×10^{-6}	2.14
54	-5.30×10^{-4}	-4.21×10^{-5}	-4.15×10^{-6}	-9.48×10^{-7}	2.32
55	-3.24×10^{-3}	-4.09×10^{-4}	-4.37×10^{-5}	1.05×10^{-5}	1.86
56	-3.79×10^{-3}	-3.72×10^{-4}	-3.96×10^{-5}	-3.86×10^{-6}	2.12
57	-3.51×10^{-3}	-3.46×10^{-4}	-3.70×10^{-5}	-3.43×10^{-6}	2.12
58	-3.25×10^{-3}	-3.25×10^{-4}	-3.48×10^{-5}	-2.90×10^{-6}	2.10
59	-2.96×10^{-3}	-3.00×10^{-4}	-3.23×10^{-5}	-2.37×10^{-6}	2.09
60	-2.52×10^{-3}	-2.59×10^{-4}	-2.80×10^{-5}	-1.77×10^{-6}	2.08
61	-1.62×10^{-3}	-1.69×10^{-4}	-1.85×10^{-5}	-9.52×10^{-7}	2.06
62	2.51×10^{-4}	2.43×10^{-5}	2.40×10^{-6}	4.83×10^{-8}	2.12
63	2.55×10^{-3}	3.89×10^{-4}	4.18×10^{-5}	-2.44×10^{-5}	1.67
64	-2.51×10^{-3}	-2.51×10^{-4}	-2.62×10^{-5}	-1.44×10^{-6}	2.10
65	-3.20×10^{-3}	-3.02×10^{-4}	-3.19×10^{-5}	-4.10×10^{-6}	2.16
66	-3.20×10^{-3}	-3.15×10^{-4}	-3.36×10^{-5}	-3.22×10^{-6}	2.12
67	-3.11×10^{-3}	-3.14×10^{-4}	-3.38×10^{-5}	-2.54×10^{-6}	2.09
68	-2.97×10^{-3}	-3.08×10^{-4}	-3.34×10^{-5}	-1.90×10^{-6}	2.07
69	-2.68×10^{-3}	-2.85×10^{-4}	-3.12×10^{-5}	-1.09×10^{-6}	2.04
70	-1.87×10^{-3}	-2.11×10^{-4}	-2.34×10^{-5}	3.59×10^{-7}	1.99
71	3.48×10^{-4}	1.66×10^{-5}	9.35×10^{-7}	1.61×10^{-7}	2.78
72	3.27×10^{-3}	6.20×10^{-4}	6.65×10^{-5}	$\mathbf{-7.99 \times 10^{-5}}$	**1.42**
73	-2.20×10^{-4}	-1.81×10^{-4}	-1.59×10^{-5}	$\mathbf{-2.32 \times 10^{-4}}$	**−1.31**
74	-2.42×10^{-3}	-2.69×10^{-4}	-2.82×10^{-5}	2.20×10^{-6}	1.99
75	-2.38×10^{-3}	-2.92×10^{-4}	-3.12×10^{-5}	6.06×10^{-6}	1.89
76	-2.40×10^{-3}	-3.07×10^{-4}	-3.32×10^{-5}	7.91×10^{-6}	1.85
77	-2.46×10^{-3}	-3.27×10^{-4}	-3.57×10^{-5}	1.04×10^{-5}	1.81
78	-2.52×10^{-3}	-3.54×10^{-4}	-3.90×10^{-5}	1.45×10^{-5}	1.76
79	-2.49×10^{-3}	-3.81×10^{-4}	-4.24×10^{-5}	2.23×10^{-5}	1.67
80	-1.09×10^{-3}	-3.51×10^{-4}	-3.99×10^{-5}	$\mathbf{1.83 \times 10^{-4}}$	**0.79**
81	1.34×10^{-3}	1.55×10^{-4}	1.55×10^{-5}	-3.32×10^{-6}	1.94

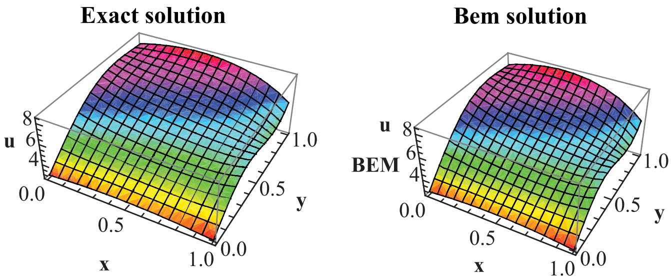

Figure 2. *Mathematica* plots of the exact and boundary element method (BEM) interior potential for the first test problem, $u(x, y) = \pi e^y \cos(x - \pi/7) + e^{(1-\pi x)} \cos(\pi y - \pi/2) + (1/100)\pi e^{5x} \cos(5y - \pi/2)$.

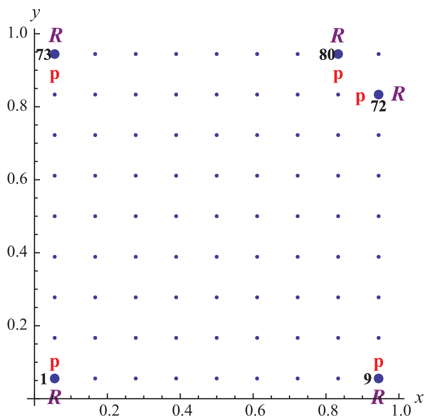

Figure 3. Interior nodes at which Richardson extrapolation potential is bad (R), compared with interior nodes at which the p-values predict bad Richardson extrapolation results (p) for the first test problem, $u(x, y) = \pi e^y \cos(x - \pi/7) + e^{(1-\pi x)} \cos(\pi y - \pi/2) + (1/100)\pi e^{5x} \cos(5y - \pi/2)$.

generally closest to the exact values. In particular, see the data in bold font in Table 1. The node numbers in bold font indicate that at each of these nodes there is a bad Richardson extrapolation result, bad p-value, or both, depending upon which data are in bold font in the table.

The numerical justification for the application of Richardson extrapolation, with the expectation that Richardson extrapolation will improve the numerical result, is provided most clearly by Table 1 and Figure 1. The Richardson extrapolation results should be better than the fine grid results. However, the Richardson extrapolation results at the nine boundary nodes numbered 10, 17, 18, 21, 22, 23, 27, 28, and 36 are not as accurate as the corresponding fine grid results. This is known here since a test problem with a known solution is used. However, in an actual application, this information would be desired, but not available. The utility of the numerical p-value estimates can now be demonstrated. These *a posteriori* estimates are available and predict the locations of bad Richardson extrapolation results. In Figure 1, it can be observed that there are bad p-values at the 10 boundary nodes numbered 1, 9, 10, 17, 18, 19, 21, 27, 28, and 36. The p-values predict the locations at which the Richardson extrapolation results are bad.

There are discrepancies, though, at the following boundary nodes. Boundary nodes numbered 1, 9, and 19 are detected as bad by the p-value estimates but are not bad Richardson nodes. However, this is desirable because, although the magnitude of the Richardson extrapolation error is smaller than the fine grid errors at these boundary nodes, both the fine grid results and the Richardson extrapolation results are very inaccurate (Richardson extrapolation does not apply). Note from Figure 1 that these boundary nodes that have been detected are at or near corners of the domain,

Table 3. Table of normal boundary flux errors and p-estimates for the second test problem, $u(x, y) = xy$.

	Normal boundary flux errors				
	nxnodes				
Node #	10	28	82	Richardson extrapolation	p-Estimate
1	-4.66×10^{-2}	-5.55×10^{-2}	-5.55×10^{-2}	$\mathbf{-5.55 \times 10^{-2}}$	5.14
2	2.92×10^{-4}	9.77×10^{-5}	1.36×10^{-5}	$\mathbf{-5.07} \times 10^{\mathbf{-5}}$	$\mathbf{7.6 \times 10^{-1}}$
3	6.34×10^{-4}	8.97×10^{-5}	1.39×10^{-5}	1.68×10^{-6}	1.79
4	6.23×10^{-4}	1.02×10^{-4}	1.67×10^{-5}	-1.54×10^{-7}	1.64
5	7.57×10^{-4}	1.33×10^{-4}	2.23×10^{-5}	-1.49×10^{-6}	1.58
6	1.1×10^{-3}	1.95×10^{-4}	3.33×10^{-5}	-1.8×10^{-6}	1.57
7	1.37×10^{-3}	3.34×10^{-4}	5.8×10^{-5}	-4.21×10^{-5}	1.2
8	1.21×10^{-2}	7.62×10^{-4}	1.35×10^{-4}	9.88×10^{-5}	2.64
9	-1.04	-9.32×10^{-1}	-9.44×10^{-1}	-9.43×10^{-1}	**2.06 + 2.86 i**
10	3.92×10^{-2}	5.46×10^{-3}	1.08×10^{-3}	4.3×10^{-4}	1.86
11	4.83×10^{-3}	9.49×10^{-4}	1.43×10^{-4}	-6.78×10^{-5}	1.43
12	1.91×10^{-3}	2.84×10^{-4}	4.25×10^{-5}	4.62×10^{-7}	1.74
13	3.08×10^{-4}	3.77×10^{-5}	4.58×10^{-6}	-6.06×10^{-8}	1.91
14	-7.57×10^{-4}	-1.33×10^{-4}	-2.23×10^{-5}	1.49×10^{-6}	1.58
15	-2.03×10^{-3}	-3.35×10^{-4}	-5.46×10^{-5}	9.34×10^{-7}	1.64
16	-3.91×10^{-3}	-7.07×10^{-4}	-1.14×10^{-4}	2.01×10^{-5}	1.54
17	-1.72×10^{-2}	-1.81×10^{-3}	-2.92×10^{-4}	-1.27×10^{-4}	2.11
18	4.89×10^{-2}	-1.77×10^{-2}	-1.91×10^{-3}	$\mathbf{-4.93 \times 10^{-3}}$	**1.31 + 2.86 i**
19	-6.62×10^{-3}	-7.32×10^{-2}	-5.75×10^{-2}	$\mathbf{-6.05 \times 10^{-2}}$	**1.31 + 2.86 i**
20	-1.72×10^{-2}	-1.81×10^{-3}	-2.92×10^{-4}	-1.27×10^{-4}	2.11
21	-3.91×10^{-3}	-7.07×10^{-4}	-1.14×10^{-4}	2.01×10^{-5}	1.54
22	-2.03×10^{-3}	-3.35×10^{-4}	-5.46×10^{-5}	9.34×10^{-7}	1.64
23	-7.57×10^{-4}	-1.33×10^{-4}	-2.23×10^{-5}	1.49×10^{-6}	1.58
24	3.08×10^{-4}	3.77×10^{-5}	4.58×10^{-6}	-6.06×10^{-8}	1.91
25	1.91×10^{-3}	2.84×10^{-4}	4.25×10^{-5}	4.62×10^{-7}	1.74
26	4.83×10^{-3}	9.49×10^{-4}	1.43×10^{-4}	-6.78×10^{-5}	1.43
27	1.09	1.06	1.06	1.06	1.86
28	-9.71×10^{-2}	1.22×10^{-2}	8.03×10^{-4}	$\mathbf{1.87 \times 10^{-3}}$	**2.06 + 2.86 i**
29	1.21×10^{-2}	7.62×10^{-4}	1.35×10^{-4}	9.88×10^{-5}	2.64
30	1.37×10^{-3}	3.34×10^{-4}	5.8×10^{-5}	-4.21×10^{-5}	1.2
31	1.1×10^{-3}	1.95×10^{-4}	3.33×10^{-5}	-1.8×10^{-6}	1.57
32	7.57×10^{-4}	1.33×10^{-4}	2.23×10^{-5}	-1.49×10^{-6}	1.58
33	6.23×10^{-4}	1.02×10^{-4}	1.67×10^{-5}	-1.54×10^{-7}	1.64
34	6.34×10^{-4}	8.97×10^{-5}	1.39×10^{-5}	1.68×10^{-6}	1.79
35	2.92×10^{-4}	9.77×10^{-5}	1.36×10^{-5}	$\mathbf{-5.07 \times 10^{-5}}$	$\mathbf{7.6 \times 10^{-1}}$
36	8.96×10^{-3}	5.45×10^{-5}	2.31×10^{-5}	2.3×10^{-5}	5.14

and these are points at which the boundary element results themselves are inaccurate. Therefore, it is good that the p-values detected these boundary nodes, and local grid refinement could be performed near these nodes in order to improve the accuracy of the boundary element results.

On the other hand, in Figure 1, it can be observed that at boundary nodes numbered 22 and 23, the p-value estimates do not predict anything problematic; however, these are bad Richardson extrapolation nodes. This is not troublesome because both the fine grid normal boundary flux results and the Richardson extrapolation normal boundary flux results are relatively accurate and the differences in relative accuracy are not significant.

5.1.2 *Richardson extrapolation for the first test problem interior potential*

The numerical results for the interior potential errors (not relative errors) computed with the coarse grid (nxnodes = nynodes = 10), intermediate grid (nxnodes = nynodes = 28), fine grid (nxnodes = nynodes = 82), and associated Richardson extrapolation and the resulting numerical estimates for the p-values are given in Table 2.

Mathematica graphics of the solution for the interior potential obtained from the Richardson extrapolation interior potential results and the exact solution are displayed in Figure 2.

The numerical results for the interior potential obtained from executing the *Mathematica* boundary element notebook three times, using the coarse, intermediate, and refined boundary grids, are compared with the Richardson extrapolation result that is computed using these three data sets at the end of the calculations (i.e. the Richardson extrapolation for the normal boundary flux is *not* used here). These four numerical approximations for the interior potential are then compared with the exact solution values at the selected interior nodes. Specifically, the Richardson extrapolation results should be compared with the results from the fine grid to see which are generally closest to the exact values. In particular, see the data in bold font in Table 2. Again, the node numbers in bold font indicate that at these nodes there is a bad Richardson extrapolation result, bad p-value, or both, depending upon which data are in bold font in the table.

The numerical justification for the application of Richardson extrapolation, with the expectation that Richardson extrapolation will improve the numerical result, is provided most clearly by Table 2 and Figure 3. The Richardson extrapolation results should be better than the fine grid results. However, the Richardson extrapolation results at the five interior nodes numbered 1, 9, 72, 73, and 80 are not as accurate as the corresponding fine grid results. This is known here since a test problem with a known solution is used. However, in an actual application, this information would be desired, but not available. Again, this demonstrates the utility of the numerical p-value estimates. These *a posteriori* estimates are available and predict the locations of bad Richardson extrapolation results. In Figure 3, it can be observed that there are bad p-values at the five interior nodes numbered 1, 9, 72, 73, and 80. The p-values predict the locations at which the Richardson extrapolation results are bad.

For this numerical example, the interior nodes at which the Richardson extrapolation values are bad and the interior nodes at which the p-value estimates predict bad Richardson extrapolation results turn out to coincide. Further, these interior nodes are all near corners of the domain, where the boundary element method performs poorly. Therefore, the p-values again can serve as *a posteriori* warning flags, i.e. indicators that the Richardson extrapolation results are suspect. In such cases, the grid can be locally refined or some other corrective action can be taken.

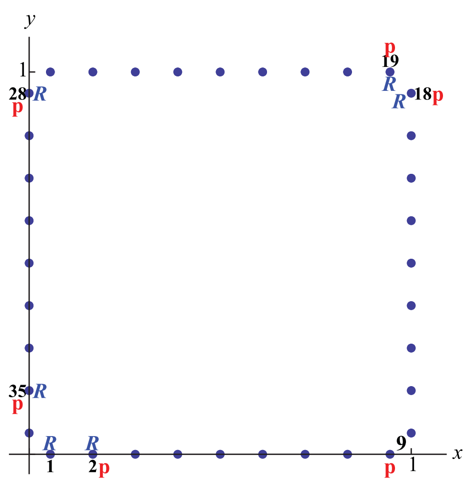

Figure 4. Boundary flux nodes at which Richardson extrapolation normal boundary flux is bad (R), compared with boundary nodes at which the p-values predict bad Richardson extrapolation results (p) for the second test problem, $u(x, y) = xy$.

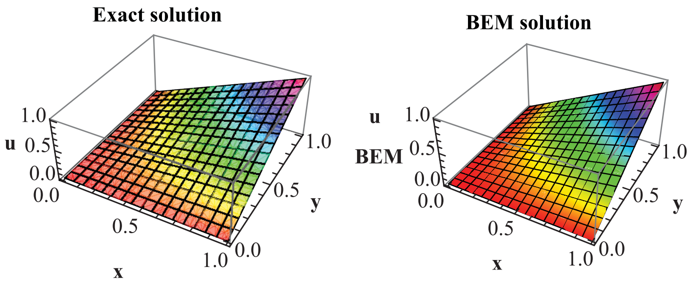

Figure 5. *Mathematica* plots of the exact and BEM interior potential for the second test problem, $u(x, y) = xy$.

5.2 *A second test problem*

5.2.1 *Richardson extrapolation for the second test problem normal boundary flux and interior potential*

The second test problem chosen for the model problem (1) has the exact solution

$$u(x, y) = xy.$$

As with the first test problem, the domain is the square $D = \{(x, y)|\ 0 < x < 1,\ 0 < y < 1\}$. The Dirichlet boundary data used were that given on the boundary by the exact solution. The numerical results for the second test problem exhibited the same type of behaviours of interest as observed for the first test problem and, therefore, will be discussed only briefly. The corresponding

Table 4. Table of interior potential errors and p-estimates for the second test problem, $u(x, y) = xy$.

	Interior potential errors				
	nxnodes				
Node #	10	28	82	Richardson extrapolation	p-Estimate
1	-1.46×10^{-5}	4.35×10^{-7}	5.45×10^{-9}	$\mathbf{1.74 \times 10^{-8}}$	$\mathbf{3.23 + 2.86\,i}$
2	6.25×10^{-6}	5.13×10^{-8}	5.76×10^{-10}	1.58×10^{-10}	4.37
3	7.32×10^{-7}	8.61×10^{-9}	4.73×10^{-12}	$\mathbf{-9.89 \times 10^{-11}}$	4.03
4	9.3×10^{-8}	-3.35×10^{-9}	-2.16×10^{-10}	$\mathbf{-3.15 \times 10^{-10}}$	$\mathbf{3.12 + 2.86\,i}$
5	-4.64×10^{-7}	-1.42×10^{-8}	-5.2×10^{-10}	-8.91×10^{-11}	3.18
6	-1.71×10^{-6}	-3.78×10^{-8}	-1.26×10^{-9}	-4.48×10^{-10}	3.48
7	-3.13×10^{-6}	-1.16×10^{-7}	-3.66×10^{-9}	6.67×10^{-10}	3
8	-7.49×10^{-5}	-5.57×10^{-7}	-1.58×10^{-8}	-1.18×10^{-8}	4.48
9	1.36×10^{-4}	-4.64×10^{-6}	-1.34×10^{-7}	$\mathbf{-2.74 \times 10^{-7}}$	$\mathbf{3.13 + 2.86\,i}$
10	6.25×10^{-6}	5.13×10^{-8}	5.76×10^{-10}	1.58×10^{-10}	4.37
11	3.6×10^{-6}	4.14×10^{-8}	3.51×10^{-10}	-1.28×10^{-10}	4.06
12	1.28×10^{-6}	9.42×10^{-9}	-1.55×10^{-10}	$\mathbf{-2.28 \times 10^{-10}}$	4.45
13	-3.49×10^{-8}	-1.11×10^{-8}	-5.75×10^{-10}	$\mathbf{7.81 \times 10^{-9}}$	$\mathbf{7.44 \times 10^{-1}}$
14	-1.22×10^{-6}	-3.43×10^{-8}	-1.22×10^{-9}	-2.74×10^{-10}	3.26
15	-3.36×10^{-6}	-8.06×10^{-8}	-2.66×10^{-9}	-7.61×10^{-10}	3.4
16	-8.61×10^{-6}	-1.91×10^{-7}	-6.17×10^{-9}	-2.01×10^{-9}	3.47
17	-1.62×10^{-5}	-4.23×10^{-7}	-1.4×10^{-8}	-3.05×10^{-9}	3.32
18	1.31×10^{-5}	-3.26×10^{-7}	-1.47×10^{-8}	$\mathbf{-2.17 \times 10^{-8}}$	$\mathbf{3.43 + 2.86\,i}$
19	7.32×10^{-7}	8.61×10^{-9}	4.73×10^{-12}	$\mathbf{-9.89 \times 10^{-11}}$	4.03
20	1.28×10^{-6}	9.42×10^{-9}	-1.55×10^{-10}	$\mathbf{-2.28 \times 10^{-10}}$	4.45
21	5.57×10^{-7}	-2.78×10^{-9}	-4.34×10^{-10}	$\mathbf{-4.44 \times 10^{-10}}$	$\mathbf{4.98 + 2.86\,i}$
22	-2.73×10^{-7}	-1.64×10^{-8}	-7.37×10^{-10}	2.86×10^{-10}	2.54
23	-1.19×10^{-6}	-3.46×10^{-8}	-1.23×10^{-9}	-2.46×10^{-10}	3.23

(*Continued*)

Table 4. Continued

	Interior potential errors				
	nxnodes				
Node #	10	28	82	Richardson extrapolation	p-Estimate
24	-2.58×10^{-6}	-6.73×10^{-8}	-2.26×10^{-9}	-5.28×10^{-10}	3.33
25	-4.43×10^{-6}	-1.22×10^{-7}	-4.08×10^{-9}	-7.69×10^{-10}	3.28
26	-4.25×10^{-6}	-1.66×10^{-7}	-5.82×10^{-9}	7.29×10^{-10}	2.95
27	-3.41×10^{-7}	-8.45×10^{-8}	-3.4×10^{-9}	**3.41×10^{-8}**	**1.05**
28	9.3×10^{-8}	-3.35×10^{-9}	-2.16×10^{-10}	**-3.15×10^{-10}**	**$3.12 + 2.86\,i$**
29	-3.49×10^{-8}	-1.11×10^{-8}	-5.75×10^{-10}	**7.68×10^{-9}**	**7.44×10^{-1}**
30	-2.73×10^{-7}	-1.64×10^{-8}	-7.37×10^{-10}	2.86×10^{-10}	2.54
31	-4.71×10^{-7}	-1.83×10^{-8}	-7.32×10^{-10}	-1.89×10^{-11}	2.96
32	-6.75×10^{-7}	-2.03×10^{-8}	-7.3×10^{-10}	-1.38×10^{-10}	3.19
33	-9.97×10^{-7}	-2.78×10^{-8}	-9.33×10^{-10}	-1.63×10^{-10}	3.26
34	-1.3×10^{-6}	-4.13×10^{-8}	-1.39×10^{-9}	-9.83×10^{-11}	3.14
35	-1.01×10^{-6}	-4.67×10^{-8}	-1.65×10^{-9}	5.49×10^{-10}	2.79
36	-8.68×10^{-8}	-2.1×10^{-8}	-8.15×10^{-10}	**8.23×10^{-9}**	**1.08**
37	-4.64×10^{-7}	-1.42×10^{-8}	-5.2×10^{-10}	-8.88×10^{-11}	3.18
38	-1.22×10^{-6}	-3.43×10^{-8}	-1.22×10^{-9}	-2.73×10^{-10}	3.26
39	-1.19×10^{-6}	-3.46×10^{-8}	-1.23×10^{-9}	-2.49×10^{-10}	3.23
40	-6.75×10^{-7}	-2.03×10^{-8}	-7.3×10^{-10}	-1.38×10^{-10}	3.19
41	0	0	-2.78×10^{-17}	0	Indeterminate
42	6.75×10^{-7}	2.03×10^{-8}	7.3×10^{-10}	1.38×10^{-10}	3.19
43	1.19×10^{-6}	3.46×10^{-8}	1.23×10^{-9}	2.8×10^{-10}	3.23
44	1.22×10^{-6}	3.43×10^{-8}	1.22×10^{-9}	2.78×10^{-10}	3.26
45	4.64×10^{-7}	1.42×10^{-8}	5.2×10^{-10}	2.49×10^{-11}	3.18
46	-1.71×10^{-6}	-3.78×10^{-8}	-1.26×10^{-9}	-4.48×10^{-10}	3.48
47	-3.36×10^{-6}	-8.06×10^{-8}	-2.66×10^{-9}	-7.61×10^{-10}	3.4
48	-2.58×10^{-6}	-6.73×10^{-8}	-2.26×10^{-9}	-5.29×10^{-10}	3.33
49	-9.97×10^{-7}	-2.78×10^{-8}	-9.33×10^{-10}	-1.78×10^{-10}	3.26
50	6.75×10^{-7}	2.03×10^{-8}	7.3×10^{-10}	1.38×10^{-10}	3.19
51	2.46×10^{-6}	7.39×10^{-8}	2.6×10^{-9}	4.11×10^{-10}	3.2
52	4.15×10^{-6}	1.25×10^{-7}	4.39×10^{-9}	6.61×10^{-10}	3.19
53	4.4×10^{-6}	1.38×10^{-7}	4.88×10^{-9}	5.58×10^{-10}	3.15
54	1.71×10^{-6}	6.21×10^{-8}	2.29×10^{-9}	1.39×10^{-11}	3.02
55	-3.13×10^{-6}	-1.16×10^{-7}	-3.66×10^{-9}	6.67×10^{-10}	3
56	-8.61×10^{-6}	-1.91×10^{-7}	-6.17×10^{-9}	-2.01×10^{-9}	3.47
57	-4.43×10^{-6}	-1.22×10^{-7}	-4.08×10^{-9}	-7.71×10^{-10}	3.28
58	-1.3×10^{-6}	-4.13×10^{-8}	-1.39×10^{-9}	-8.69×10^{-11}	3.14
59	1.19×10^{-6}	3.46×10^{-8}	1.23×10^{-9}	2.3×10^{-10}	3.23
60	4.15×10^{-6}	1.25×10^{-7}	4.39×10^{-9}	6.61×10^{-10}	3.19
61	8.3×10^{-6}	2.46×10^{-7}	8.59×10^{-9}	1.36×10^{-9}	3.21
62	1.16×10^{-5}	3.48×10^{-7}	1.21×10^{-8}	1.79×10^{-9}	3.19
63	2.74×10^{-6}	1.92×10^{-7}	7.06×10^{-9}	**-7.37×10^{-9}**	**2.39**
64	-7.49×10^{-5}	-5.57×10^{-7}	-1.58×10^{-8}	-1.18×10^{-8}	4.48
65	-1.62×10^{-5}	-4.23×10^{-7}	-1.4×10^{-8}	-3.05×10^{-9}	3.32
66	-4.25×10^{-6}	-1.66×10^{-7}	-5.82×10^{-9}	7.29×10^{-10}	2.95
67	-1.01×10^{-6}	-4.67×10^{-8}	-1.65×10^{-9}	5.65×10^{-10}	2.79
68	1.22×10^{-6}	3.43×10^{-8}	1.22×10^{-9}	2.54×10^{-10}	3.26
69	4.4×10^{-6}	1.38×10^{-7}	4.88×10^{-9}	5.58×10^{-10}	3.15
70	1.16×10^{-5}	3.48×10^{-7}	1.21×10^{-8}	1.79×10^{-9}	3.19
71	2.88×10^{-5}	8.05×10^{-7}	2.76×10^{-8}	5.33×10^{-9}	3.26
72	5.55×10^{-5}	8.32×10^{-7}	2.99×10^{-8}	1.8×10^{-8}	3.84
73	1.36×10^{-4}	-4.64×10^{-6}	-1.34×10^{-7}	**-2.74×10^{-7}**	**$3.13 + 2.86\,i$**
74	1.31×10^{-5}	-3.26×10^{-7}	-1.47×10^{-8}	**-2.17×10^{-8}**	**$3.43 + 2.86\,i$**
75	-3.41×10^{-7}	-8.45×10^{-8}	-3.4×10^{-9}	**3.42×10^{-8}**	**1.05**
76	-8.68×10^{-8}	-2.1×10^{-8}	-8.15×10^{-10}	**8.23** $\times 10^{-9}$	**1.08**
77	4.64×10^{-7}	1.42×10^{-8}	5.2×10^{-10}	1.52×10^{-10}	3.18
78	1.71×10^{-6}	6.21×10^{-8}	2.29×10^{-9}	1.39×10^{-11}	3.02
79	2.74×10^{-6}	1.92×10^{-7}	7.06×10^{-9}	**-7.37×10^{-9}**	**2.39**
80	5.55×10^{-5}	8.32×10^{-7}	2.99×10^{-8}	1.8×10^{-8}	3.84
81	-2.57×10^{-4}	8.84×10^{-6}	2.62×10^{-7}	**5.31×10^{-7}**	**$3.12 + 2.86\,i$**

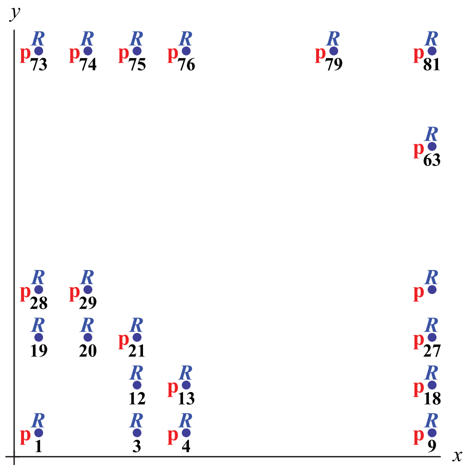

Figure 6. Interior nodes at which Richardson extrapolation potential is bad (R), compared with interior nodes at which the p-values predict bad Richardson extrapolation results (p) for the second test problem, $u(x, y) = xy$.

numerical and graphical results are displayed, respectively, in Table 3, Figures 4 and 5, Table 4, and Figure 6. As for the first test problem, the node numbers and data in Tables 3 and 4 in bold font indicate that at each of these nodes there is a bad Richardson extrapolation result, bad p-value, or both, depending upon which data are in bold font in the table. In this example, the arbitrary p cut-off values were selected as 1 for the normal boundary flux data and 2.5 for the interior potential data. Using these values, the bad p-value nodes predicted the bad Richardson extrapolation nodes fairly well, but with discrepancies, as will now be addressed.

The normal boundary flux at boundary node number 1 exhibits a bad Richardson value, but not a bad p-value. This is not troublesome because both the fine grid normal boundary flux results and the Richardson extrapolation normal boundary flux results are relatively accurate (for values near corners) and the difference in values is not significant. At boundary node number 9, the interior potential has a bad p-value, although the Richardson extrapolation result is more accurate than the corresponding fine grid result. However, at this node both the fine grid and Richardson extrapolation results are quite inaccurate. Therefore, it is good that the p-value detected this boundary node as a node at which the Richardson extrapolation result (and fine grid result) is invalid and should be rejected.

The interior potential at interior nodes numbered 3, 12, 19, and 20 exhibit bad Richardson values, but not bad p-values. Again, this is not troublesome because both the fine grid normal boundary flux results and the Richardson extrapolation normal boundary flux results are relatively accurate and the differences between them are not significant.

Observe that again, as demonstrated by this second test problem, the p-values can serve as *a posteriori* warning flags, i.e. indicators that the Richardson extrapolation results at specific grid points are not valid.

6. Conclusions

Richardson extrapolation was used to improve the accuracy of the numerical solutions for the normal boundary flux and for the interior potential resulting from the boundary element method. Some theoretical justifications were provided for the case of a smooth boundary and smooth functions. The orders of dominant error terms were estimated numerically, and these estimates were then used to develop an *a posteriori* technique to predict if the Richardson extrapolation results are reliable. Numerical results for test problems were presented to demonstrate the technique.

Acknowledgements

The author acknowledges support to write the *Mathematica* notebook implementing the boundary element method from a University of Tulsa Faculty Summer Fellowship. The author thanks the referees for their comments.

References

[1] K. Atkinson and W. Han, *Theoretical Numerical Analysis – A Functional Analysis Framework*, Springer-Verlag, New York, 2001, Sections 11.1–11.2, pp. 342–362; Chapter 12, pp. 405–435.
[2] R.L. Burden and J.D. Faires, *Numerical Analysis*, 8th ed., Thomson, Brooks/Cole, Boston, MA, 2005, Section 2.5, pp. 83–87; Section 4.2, pp. 179–186.
[3] C. Constanda, *Direct and Indirect Boundary Integral Equation Methods*, Chapman & Hall/CRC, Boca Raton, FL, 2000, Chapter 1, pp. 1–53.
[4] L. Gaul, M. Kogl, and M. Wagner, *Boundary Element Methods for Engineers and Scientists*, Springer, Berlin, 2003.
[5] L. Kaitai and Y. Ningning, *The Extrapolation Method for Boundary Finite Elements*, IMA Preprint Series, #287, January, 1987. Available at http://ima.umn.edu/preprints/Jan87-Dec87/287.pdf.
[6] Y. Ning and L. Kai-tai, *An extrapolation method for BEM*, J. Comput. Math. 7(2) (1989), pp. 217–225.
[7] M. Panahi, *The boundary element method for numerical solution of the Laplace equation*, Int. J. Appl. Math. 19(4) (2006), pp. 403–410.
[8] U. Rüde and A. Zhou, *Multi-parameter extrapolation methods for boundary integral equations*, Adv. Comput. Math. 9 (1998), pp. 173–190.
[9] G.D. Smith, *Numerical Solution of Partial Differential Equations: Finite Difference Methods*, 3rd ed., Oxford University Press, Oxford, 1987, p. 249.
[10] Y. Xu and Y. Zhao, *An extrapolation method for a class of boundary integral equations*, Math. Comp. 65(214) (1996), pp. 587–610.
[11] Y. Yan, *The collocation method for first-kind boundary integral equations on polygonal regions*, Math. Comp. 54(189) (1990), pp. 139–154.
[12] Y. Yan and I.H. Sloan, *On integral equations of the first kind with logarithmic kernels*, J. Integral Equ. Appl. 1 (1988), pp. 549–579.